



Cite this: *Green Chem.*, 2023, **25**, 1424

Valorization of chicken feathers using aqueous solutions of ionic liquids†

Cariny Polesca,^a Helena Passos,^a Bruno M. Neves,^b João A. P. Coutinho^a and Mara G. Freire^{a*}

The poultry-processing industry generates large quantities of waste rich in keratin, a fibrous protein representing around 90 wt% of chicken feathers, which is currently disposed of by landfilling or incineration. Keratin is commonly recognized as a renewable biopolymer resource used in the preparation of biomaterials (e.g., films and hydrogels) of interest in biomedical applications. Even though research on keratin recovery from chicken feathers started many years ago, very few keratin materials from this source have been developed due to keratin's low solubility in most common solvents and poor protein recovery yield. Although ionic liquids (ILs) have been reported as alternative solvents with high dissolution capability for several biopolymers, keratin recovery from chicken feathers using aqueous solutions of ILs has not been investigated to date. Considering the Green Chemistry Principles (especially the first one: zero waste) and circular economy concepts, in this work, we show that chicken feathers can be effectively dissolved in an aqueous solution of 1-butyl-3-methylimidazolium acetate (80 wt%), greatly enabling keratin recovery and preparation of keratin biofilms. Keratin recovery from the IL aqueous solution was optimized considering the coagulant type, solution:coagulant weight ratio, temperature, and time, with the coagulant type being the variable with higher influence on the recovery process. Under the best conditions (ethanol, 1:2 w/w, 5 °C, and 1 h), 90 wt% of keratin was recovered. IL recovery and reuse were also evaluated, and 82 wt% of recovery yield was achieved at the end of the third cycle. The recovered keratin was characterized, confirming the required physicochemical properties. A keratin film was finally prepared and characterized through cell viability, oxidative stress and wound healing assays, opening the path for the use of keratin films in biomedical applications.

Received 24th November 2022,
Accepted 17th January 2023

DOI: 10.1039/d2gc04477c

rsc.li/greenchem

Introduction

Chicken is one of the most consumed meats in the world, with an annual consumption of 65 million tons worldwide. Its high consumption produces a large amount of feather waste, corresponding to around 7 wt% of the total mass of an adult chicken.^{1–6} Currently, this waste is disposed of through incineration or landfilling, contributing to environmental pollution and highlighting the necessity to develop sustainable and profitable ways of waste valorization^{1,7} that are connected to the biorefinery concept.⁸ On this subject, it is crucial to highlight the circular economy concept, considered to be a top priority in the EU Sustainable Development Goals (SDGs).⁸

On a dry weight basis, the highest component in chicken feathers is keratin (around 90 wt%), with the rest consisting of fibers, ash, and fat.⁹ Keratin is a structural and fibrous protein, and the third most abundant biopolymer in the environment, after cellulose and chitin.^{10–13} Keratin is also the main component of hair, wool, nails, hooves, and horns. Nevertheless, the potential production of this protein from chicken feathers is 2.5 times higher than the current output of wool (the main source investigated in the literature).⁶ Due to its properties, keratin has applications in the biomedical field and tissue engineering,¹⁴ encouraging some researchers to investigate its use for the preparation of biomaterials (e.g., films and hydrogels).^{15–17}

Despite its relevance, due to the inter- and intramolecular disulfide bonds in sulfur-containing amino acids, keratin shows low solubility in common organic solvents and has a poor recovery yield.^{10,13,18,19} Furthermore, commonly reported methods (e.g., chemical hydrolysis, microwave, and steam exposure techniques) exert negative impacts on the protein structure and respective properties. For instance, the elevated temperatures used in the chemical hydrolysis method promote

^aCICECO – Aveiro Institute of Materials, Department of Chemistry, University of Aveiro, 3810-193 Aveiro, Portugal. E-mail: maragfreire@ua.pt

^bDepartment of Medical Sciences and Institute of Biomedicine-iBiMED, University of Aveiro, 3810-193 Aveiro, Portugal

† Electronic supplementary information (ESI) available. See DOI: <https://doi.org/10.1039/d2gc04477c>



amino acid degradation, and methods using chemical compounds (e.g., thiols and 2-mercaptoethanol) are time-consuming and present environmental harm, as reviewed by Chilakamarry *et al.*¹¹ and Shavandi *et al.*²⁰ To overcome this concern, several studies have been conducted to identify efficient and greener alternatives to completely dissolve biomass rich in keratin and achieve efficient keratin recovery. Among the alternatives reported, the use of ionic liquids (ILs) – salts composed of large organic cations and organic or inorganic anions – should be highlighted.^{10,21–27} When properly designed, ILs allow complete biomass dissolution without requiring high temperatures and long processing times. Another disadvantage overcome by the use of ILs is in the keratin recovery process. Traditionally, when conventional dissolution (e.g., using urea and sodium metabisulfite) is carried out, either dialysis²⁸ or an adjustment of the isoelectric point using hydrochloric acid along with sodium sulfate^{6,12} is necessary to recover keratin. When using ILs for biopolymer recovery, coagulant solvents, such as water²² or ethanol,²⁹ can be used.

In 2005, 1-butyl-3-methylimidazolium chloride ([C₄C₁im]Cl) was used to dissolve wool and regenerate wool keratin for the first time,²⁵ and since then ILs have demonstrated excellent results with this type of biomass when properly selected.^{20,23,29,30} Due to the wide variety of ILs and the complexity of keratin (which does not have regular repeating units), it is not easy to identify the best IL for keratin dissolution. To illustrate this, Liu *et al.*¹⁰ screened 621 ILs for the dissolution of three keratin models using COSMO-RS and validated it with experimental results. According to the authors, 1-ethyl-3-methylimidazolium acetate ([C₂C₁im][C₁CO₂]) was one of the best ILs for protein dissolution, in accordance with the results reported by Zhang *et al.*,³¹ who investigated the regeneration of wool keratin using this IL. The results showed that when the same cation is used, the anion [C₁CO₂][–] presents a higher ability to dissolve keratin than Cl[–] and Br[–] due to its stronger hydrogen-bonding acceptor ability. Despite these promising results,^{10,31} keratin recovery from biomass using [C₁CO₂]-based ILs has been scarcely addressed in the literature. Wool has been the focus of most research studies involving ILs,^{17,22,25,26,32} and chicken feathers have not been efficiently used.^{23,33} Wang *et al.*³³ reported the use of a hydrophobic IL, 1-hydroxyethyl-3-methylimidazoliumbis(trifluoromethanesulfonyl)amide, and sodium bisulfite, for chicken feather dissolution, achieving a maximum yield of keratin of 21 wt%. Later, Ji *et al.*²³ investigated the use of some imidazolium-based ILs and sodium sulfite for keratin recovery from duck feathers, achieving a yield of 75.1 wt%. In both works, sodium sulfite salts were used to improve biomass dissolution, and no pure ILs or their aqueous solutions have been reported for chicken feather dissolution and keratin recovery.

In this study, the performance of ILs and their aqueous solutions for chicken feather dissolution and keratin recovery was investigated. The keratin recovery conditions were optimized by varying the coagulant type, solution:coagulant weight ratio, temperature, and time. The physicochemical properties of the recovered keratin samples were determined. IL

recovery and reuse were also evaluated, aiming for the development of a process more interesting in terms of economic and environmental factors. Using the optimal conditions, a keratin film was prepared. Its mechanical properties and biological activity were evaluated, foreseeing biomedical applications, and opening the path to more research in this field.

Materials and methods

Materials

Chicken feathers were collected from Campoaves Company in Oliveira de Frades, Portugal. The ILs used, *viz.* 1-butyl-3-methylimidazolium acetate ([C₄C₁im][C₁CO₂]) (>98 wt%), [C₂C₁im][C₁CO₂] (>98 wt%), [C₄C₁im]Cl (99 wt%), 1-ethyl-3-methylimidazolium chloride ([C₂C₁im]Cl) (99 wt%), 1-butyl-3-methylimidazolium bromide ([C₄C₁im]Br) (99 wt%), 1-butyl-3-methylimidazolium thiocyanate ([C₄C₁im]SCN) (>98 wt%) and 1-butyl-1-methylpyrrolidinium ([C₄C₁pyrr]Cl) (99 wt%), were purchased from IOLITEC. Ethanol (99.8 wt%) and acetone (100 wt%) were acquired from Fisher Scientific and Valente & Ribeiro Lda, respectively. Chemical reagents used in sodium dodecyl sulfate-polyacrylamide gel electrophoresis (SDS-PAGE) analysis, including urea, hydrochloric acid, tris (hydroxymethyl)-aminomethane (99 wt%) and PageRuler™ Low Range Unstained Protein Ladder, were purchased from Thermo Fisher Scientific. Sodium dodecyl sulfate (SDS) and glycerol were from PanReac AppliChem and Biochem Chemopharma, respectively. TEO-Tricine Precast Gels-Run Blue™ (12 wt%, 12-well, 10 × 10 cm) was purchased from Abcam. The compounds used for biological analysis, including Roswell Park Memorial Institute (RPMI) 1640 medium, penicillin, streptomycin, lipopolysaccharide (LPS) from *Escherichia coli* (serotype 026:B6), propidium iodide (PI), and resazurin were obtained from Sigma Chemical Co. Dulbecco's Modified Eagle's Medium (DMEM), fetal bovine serum (FBS) and chloromethyl derivative of 2',7'-dichlorodihydrofluorescein diacetate (CM-H2DCFDA) were obtained from Thermo Fisher Scientific. cellQART® tissue culture treated 12-well and 24-well insert PET membranes of pore size 1 mm were acquired from SABEU GmbH & Co. KG. Anti-human CD54-APC (clone 1H4) and CD86-FITC (clone BU63) were purchased from ImmunoTools GmbH, and anti-human CD83-APC (clone HB15e) was from BD Biosciences.

Chicken feather pre-treatment

The collected feathers were washed three times with soap and dried in an air oven (Carbolite Gero) at 50 °C for 72 h. Then, the feathers were milled and immersed in ethanol 99% for 24 h to remove fatty matter. The cleaned wet feathers were dried at 50 °C for 24 h and then stored in plastic bags at 5 °C until further use.

Chicken feather dissolution and keratin recovery

IL screening for chicken feather dissolution. Seven ILs, namely [C₂C₁im]Cl, [C₂C₁im][C₁CO₂], [C₄C₁im]Cl,



$[C_4C_1im][C_1CO_2]$, $[C_4C_1im]Br$, $[C_4C_1im][SCN]$, and $[C_4C_1pyrr]Cl$, were used in an initial screening to verify the IL dissolution capability of chicken feathers. The ILs selected comprise a combination of different cations and anions, taking into consideration the ILs that have been reported in the literature for the effective dissolution of different biopolymers from biomass.^{29,31,34–37} Nevertheless, to the best of our knowledge, the selected ILs have so far not been evaluated for chicken feather dissolution. The dissolution assays were carried out at 100 °C for 4 h in a solid:liquid (chicken feathers:solvent) ratio of 1:20 w/w in a carousel (Carousel Tech, Radleys). These conditions were established according to previously reported data.^{11,23,38} Treated chicken feathers were used, as previously described. After identifying the best IL, the IL concentration effect was evaluated using pure $[C_4C_1im][C_1CO_2]$ and aqueous solutions of IL at 80 wt% and 60 wt%.

Keratin recovery. Aqueous solutions of $[C_4C_1im][C_1CO_2]$ at 80 wt% were prepared and heated at 100 °C. When this temperature was achieved, treated feathers were added to the IL solution, in a solid:liquid ratio of 1:20 w/w. The dissolution was conducted at 100 °C for 4 hours. Then, the solution was moved to a centrifuge tube. The coagulant solvent (water, ethanol, water:ethanol mixture or acetone) was added at a solution:coagulant ratio of 1:1, 1:2, 1:3 or 1:5 w/w and stored at different temperatures (−20 °C, 5 °C or 25 °C) for different time periods (from 1 h to 24 h) to induce keratin precipitation. Subsequently, the solution was centrifuged for 20 min at 25 °C and 4000 rpm in a refrigerator centrifuge machine (Neya 16 R, Remi Elektrotechnik Ltda), promoting the separation of the precipitated keratin. The obtained protein was washed with water to remove IL residues and centrifuged at the previously described conditions. Finally, the recovered keratin was dried at 50 °C for 48 h.

The keratin recovery yield (RY%) was determined from eqn (1). Contrary to what is commonly observed in the literature (keratin yield based on the total biomass mass), the yield of the recovered keratin was obtained considering the amount of protein available in chicken feathers (90 wt%).⁹ All experiments were conducted at least in duplicate, with the average values and respective standard deviation being presented.

$$RY\% = \left(\frac{m_{\text{keratin}}}{m_{\text{feathers}} \times 0.9} \right) \times 100 \quad (1)$$

where m_{keratin} represents the mass of keratin recovered and dried and m_{feathers} the mass of chicken feathers used at the dissolution step.

Keratin characterization

Sodium dodecyl sulfate-polyacrylamide gel electrophoresis (SDS-PAGE). 4 mg of the recovered keratin was dissolved in 1 mL of buffer solution (0.05 g mol^{−1} Tris-HCl pH 8.0, 8 g mol^{−1} urea, and 0.01 g mol^{−1} DTT) and stirred for 2 h. The keratin solution was dissolved in a running buffer (0.5 g mol^{−1} Tris-HCl pH 6.8, 20 w/w glycerol, 4 w/w SDS, and 0.01 g mol^{−1} dithiothreitol (DTT)) and then heated at 90 °C for 5 min to

complete denaturation. The protein marker (3.4 to 100 kDa) and the samples were loaded into the polyacrylamide gels and subjected to a run at 80 V for 1 h, followed by 1 h at 120 V. Then, the proteins were stained with Coomassie brilliant blue G-250 overnight at room temperature.

Fourier transform infrared attenuated total reflectance (FTIR-ATR). The FTIR-ATR spectra of chicken feathers and recovered keratin samples were acquired in a FTIR system Spectrum BX, PerkinElmer, equipped with a single horizontal Golden Gate ATR cell and a diamond crystal. The analysis of functional groups available was performed at room temperature with controlled air humidity. All data were recorded in a frequency range of 4000–400 cm^{−1} by accumulating 32 scans with a resolution of 4 cm^{−1} and an interval of 1 cm^{−1}. The acquired spectra were recorded as absorbance values.

Thermogravimetric analysis (TGA). Thermogravimetric analyses were carried out in a differential thermogravimetric analyzer Hitachi STA300. Approximately 5 mg of keratin samples was placed in an aluminum pan and further analyzed under a nitrogen gas blanket at a flow rate of 1 mL min^{−1}. The samples were heated at a rate of 10 °C min^{−1} with a temperature range of 30–900 °C.

IL recovery and reuse

To achieve IL recovery and possible reuse, after the centrifugation step, the supernatant (solution composed of IL + water + coagulant) was collected and transferred to a clean 50 mL round bottomed flask, previously weighed. The volatile compounds were removed from the solution using a rotatory evaporator consisting of rotavapor R-10, heating bath B-491, vacuum pump V-700 and vacuum controller V-850 (all from Buchi, Switzerland). The obtained solution was dried in a vacuum line for 5 days at room temperature to remove any traces of water and coagulant. The IL acquired was weighed, and the IL recovery yield was determined from the dry IL mass and the initial IL mass used in feathers dissolution. The IL reuse was evaluated for a total of 3 dissolution and recovery cycles.

Keratin film processing

Keratin film processing was evaluated using the best conditions for keratin recovery. After the washing step, a keratin solution (15 wt%) was prepared with distilled water. The mixture was mixed under constant magnetic stirring at 60 °C for 30 min. Then, the solution was cast on silicone molding and placed in an air oven at 50 °C for 24 h.

Keratin film characterization

Scanning electron microscopy (SEM). SEM was performed using a high-resolution field-emission (HR-FESEM) Hitachi SU70 microscope. The keratin film was coated with a thin carbon layer before the sample analysis to ensure its conductivity. Images were obtained using an accelerating voltage of 10 kV and a working distance of 15 nm.

Tensile strength. Tensile strength was determined using a Lloyd EZ 50 testing machine. Film samples were cut into strips



1 cm wide and 4 cm long, and at least two replicates were performed.

Contact angle. Contact angles were determined to assess the hydrophilicity of the film using a semi-automatic wettability analysis with high dosing precision (DSA25S, Krüss). Multiple measurements were made by adding a drop of 7 μL of solvent (water or ethylene glycol) at a rate of 7 $\mu\text{L s}^{-1}$ on the film deposited on a rigid substrate.

Biological activity

Cell culture. Murine raw 264.7 macrophages (ATCC TIB-71) were cultured in DMEM containing 4.5 g L^{-1} glucose, 0.004 mol L^{-1} L-glutamine, and 1500 mg L^{-1} sodium bicarbonate supplemented with 10% non-inactivated fetal FBS, 100 U mL^{-1} penicillin and 100 $\mu\text{g mL}^{-1}$ streptomycin. The human keratinocyte cell line HaCaT (DKFZ, Heidelberg, Germany) and the mouse fibroblast cell line 3T3 (ATCC CRL1658) were cultured in the same DMEM medium containing heated inactivated FBS. These adherent cells were incubated at 37 $^{\circ}\text{C}$ in a humidified atmosphere (95% air and 5% CO_2) and were used after reaching 70%–80% confluence, which occurs approximately every 3 days after each passage. The THP-1 human monocytic cell line (ATCC TIB-202) was cultured and maintained at a cell density between 0.2×10^6 and 1×10^6 cells per mL in RPMI 1640 supplemented with 10% inactivated FBS, 0.025 g mol^{-1} glucose, 0.010 g mol^{-1} HEPES, 0.001 mol L^{-1} sodium pyruvate, 100 U mL^{-1} penicillin and 100 $\mu\text{g mL}^{-1}$ streptomycin. Cells were subcultured every 3 or 4 days and kept in culture for 2 months.

Cell viability assays. To investigate the biocompatibility of the keratin film, its effect on the viability/metabolic activity of monocytes, macrophages, keratinocytes, and fibroblasts was assessed by flow cytometry through an analysis of PI exclusion or by the resazurin assay.³⁹ For monocytes, 0.3×10^6 THP1 cells were plated in 0.5 mL of medium per well of a 24-well plate, and then the keratin film was put into contact with cell cultures for 24 h by means of transwell inserts with 1 μm PET membranes. At the end of exposure, cells were collected, washed twice with PBS, and then resuspended in 400 μL of FACS buffer (PBS + 2% FBS). 1 μL of 1 mg mL^{-1} PI was added to each culture, and cells were acquired in an Accuri C6 flow cytometer (BD Bioscience). Dead cells were identified by including PI and increased fluorescence in the FL2 channel (585/40 nm filter). For adherent cell lines, 0.5×10^6 raw 264.7, 0.1×10^6 HaCaT or 0.1×10^6 3T3 cells were plated per well of a 24-well plate in 500 mL medium and let to stabilize overnight. Then, keratin film samples were put into contact with cell cultures using transwell inserts. After 24 h of incubation, resazurin was added to cells (final concentration of 50 μM) during the last 2 h of incubation. Finally, 200 μL from each culture was transferred to a 96-well plate, and the absorbance of resorufin (the product of the resazurin reduction) was measured at 570 and 600 nm in a Tecan Infinite M200 Pro spectrophotometer (Tecan Trading AG). The data are the average of three biologically independent experiments conducted in duplicate for each culture, and the results were expressed as the average

cell viability \pm SD. The keratin film used in this study was sterilized by exposure to UV for 45 min.

Oxidative stress evaluation. To evaluate whether exposure to the keratin film triggers oxidative stress, ROS formation was analyzed with the ROS indicator CM-H2DCFDA. Briefly, 0.75×10^6 raw 264.7 cells were plated per well of a 12-well plate and let to stabilize overnight, followed by co-culture with the keratin film. As a positive control for oxidative stress induction, cells were treated with 100 ng mL^{-1} LPS. After 24 h of exposure, cells were washed with PBS and then loaded with 2 μM CM-H2DCFDA in HBSS (in mol L^{-1} : 0.0013 CaCl_2 , 0.0005 MgCl_2 , 0.0053 KCl, 0.138 NaCl, 0.00044 KH_2PO_4 , 0.0042 NaHCO_3 , and 0.00034 Na_2HPO_4 , pH 7.4) for 30 min at 37 $^{\circ}\text{C}$ in the dark. Cells were washed three times with HBSS, and images were acquired with an EVOS M5000 imaging system (Thermo Fisher Scientific) at 20 \times magnification (scale bar 100 μm).

Wound healing assays. The effect of the keratin film on the spreading and migration capabilities of HaCaT keratinocytes and 3T3 fibroblasts was assessed using a scratch wound assay which addresses the expansion of a cell population on surfaces. HaCaT or 3T3 cells were seeded into 12-well tissue culture dishes at a density of 0.3×10^6 cells per mL and let to stabilize in a medium containing 10% FBS until they reached a confluent cell monolayer. Then, a linear wound was generated in the monolayer with a sterile 200 μL or 1000 μL plastic pipette tip for HaCaT or 3T3 cells, respectively. Any cellular debris was removed by washing the wells with PBS. At least five images of the scratched area of each culture were taken at this 0 h time point using an EVOS M5000 imaging system at 4 \times magnification (scale bar 200 μm). Exposure to the keratin film was performed in a medium containing 2% FBS. Medium containing 10% FBS or cytochalasin D was used as positive and negative controls, respectively. After 16 h, at least five images of the scratched area of each condition were taken and compared to the corresponding 0 h time point.

Results and discussion

IL screening for chicken feather dissolution

Most of the investigated ILs showed no ability to achieve the complete dissolution of chicken feathers at the ratio 1 : 20 w/w, with the exception of the acetate-based ILs ($[\text{C}_4\text{C}_1\text{im}][\text{C}_1\text{CO}_2]$ and $[\text{C}_2\text{C}_1\text{im}][\text{C}_1\text{CO}_2]$) that allowed complete chicken feather dissolution at 100 $^{\circ}\text{C}$ and 4 h. This is in accordance with results previously reported in the literature since the acetate anion is a strong hydrogen bond acceptor with high hydrogen-bond basicity,³¹ thus allowing the dissolution of biopolymers that can establish hydrogen-bonding, such as proteins. Passos *et al.*⁴⁰ reported the hydrogen-bond basicity of some ILs by estimating their hydrogen bond interaction energies (E_{HB}) using COSMO-RS. ILs with more negative values of E_{HB} presented higher hydrogen bond basicity. The following order was observed for the ILs investigated in this work: $[\text{C}_2\text{C}_1\text{im}][\text{C}_1\text{CO}_2]$ ($E_{\text{HB}} = -20.21 \text{ kJ mol}^{-1}$) > $[\text{C}_4\text{C}_1\text{im}][\text{C}_1\text{CO}_2]$



($E_{\text{HB}} = -19.83 \text{ kJ mol}^{-1}$) > $[\text{C}_2\text{C}_1\text{im}]\text{Cl}$ ($E_{\text{HB}} = -14.99 \text{ kJ mol}^{-1}$) > $[\text{C}_4\text{C}_1\text{im}]\text{Cl}$ ($E_{\text{HB}} = -14.52 \text{ kJ mol}^{-1}$) > $[\text{C}_4\text{C}_1\text{im}]\text{Br}$ ($E_{\text{HB}} = -11.66 \text{ kJ mol}^{-1}$) > $[\text{C}_4\text{C}_1\text{im}][\text{SCN}]$ ($E_{\text{HB}} = -8.20 \text{ kJ mol}^{-1}$) > $[\text{C}_4\text{C}_1\text{pyrr}]\text{Cl}$ ($E_{\text{HB}} = -6.99 \text{ kJ mol}^{-1}$). Only ILs with the acetate anion are able to completely dissolve chicken feathers under the studied conditions. Furthermore, aqueous solutions of acetate-based ILs are alkaline ($\text{pH} \cong 10.4$, as determined by us), in contrast with aqueous solutions of $[\text{C}_2\text{C}_1\text{im}]\text{Cl}$ ($\text{pH} 4.77$) and $[\text{C}_4\text{C}_1\text{pyrr}]\text{Cl}$ ($\text{pH} 5.69$). These results additionally suggest that alkaline aqueous solutions show better performance in chicken feather dissolution, which has also been observed for cellulose.⁴¹ Taking these results into account and considering the similar performance of both acetate-based ILs for chicken feather dissolution, the following studies were carried out with $[\text{C}_4\text{C}_1\text{im}][\text{C}_1\text{CO}_2]$ aqueous solutions.

The IL concentration effect was evaluated using pure IL and aqueous solutions of $[\text{C}_4\text{C}_1\text{im}][\text{C}_1\text{CO}_2]$ at 80 wt%, and 60 wt%. According to the results obtained, adding water up to 20 wt% promotes viscosity reduction, accelerating the mass transfer process and facilitating feather dissolution. However, when the water concentration increases from 20 wt% to 40 wt%, the solution cannot completely dissolve the added chicken feathers (1 : 20 w/w) since water starts to compete with the hydrogen bonds responsible for dissolution, as previously reported.⁴² In summary, the maximum dissolution of chicken feathers was obtained with an aqueous solution of $[\text{C}_4\text{C}_1\text{im}][\text{C}_1\text{CO}_2]$ at 80 wt%.

Keratin recovery

The effect of the coagulant solvent and solution:coagulant ratio was evaluated for keratin recovery from IL aqueous solution, while keeping time and temperature constant at 1 h and 5 °C, respectively. The results obtained are presented in Fig. 1. Among the studied coagulants (water, ethanol, acetone, and water:ethanol mixture), acetone results in a lower keratin recovery yield, ranging from 7.74 to 10.93 wt%, while ethanol presents the best results, with recovery yields ranging from 16.62 to 90.17 wt%. Between these solvents, water resulted in yields in a range from 28.85 to 52.64 wt%, and water:ethanol mixture presented yields ranging from 21.45 to 48.82 wt%. Accordingly, it seems that the interactions established between the studied IL and ethanol are more efficient than between IL-

water and IL-acetone, leading to a more efficient protein precipitation. This is due to the hydrogen bonds formed between the hydrogen atom (–OH) of ethanol with the IL cation (H-bonding donor) and the IL anion (hydrogen-bond acceptor).⁴³

Considering ethanol as the best coagulant agent and evaluating the solution:coagulant ratio, it is possible to observe that by increasing it from 1 : 1 to 1 : 2 w/w, the keratin recovery yield increases from 16.62 to 90.17 wt%. However, no significant differences in the keratin recovery yield were observed above this ratio.

The temperature effect was also considered on the recovery yield of keratin, whose results are provided in Fig. 2. Water and ethanol were used as the coagulant agents for 1 h and at a solution:coagulant ratio of 1 : 2 w/w. Concerning the results obtained with ethanol, no significant differences were observed in the keratin recovery yield (90.17–92.86 wt%) when the temperature was changed from –20 °C to 25 °C. Nevertheless, evaluating the temperature effect for water, there is an increase of ~8 wt% (from 44.45 up to 52.64 wt%) in the keratin recovery yield when the temperature decreases from 25 °C to 5 °C.

Fig. 3 presents the behavior of the keratin recovery yield with time when water (5 °C) and ethanol (5 °C or –20 °C) were used as coagulant agents at a solution:coagulant ratio of 1 : 2 w/w. Considering the use of ethanol, no significant differences were observed from 1 h to 24 h, independently of the temperature. Thus, one hour was enough to achieve a high keratin recovery yield, *i.e.* 90.17 wt%. On the other hand, when water

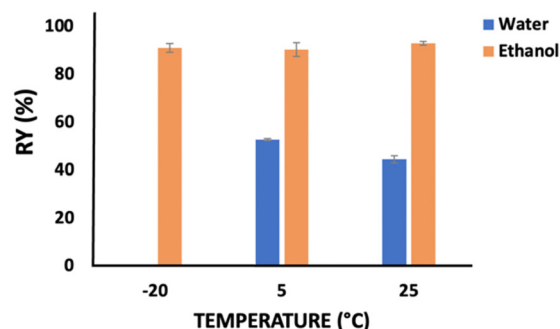


Fig. 2 Temperature effect on the keratin recovery yield.

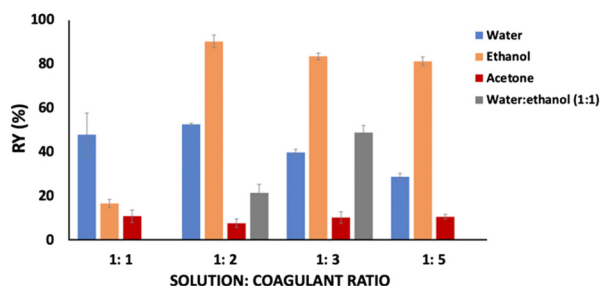


Fig. 1 Coagulant and solution:coagulant ratio effect on the keratin recovery yield.

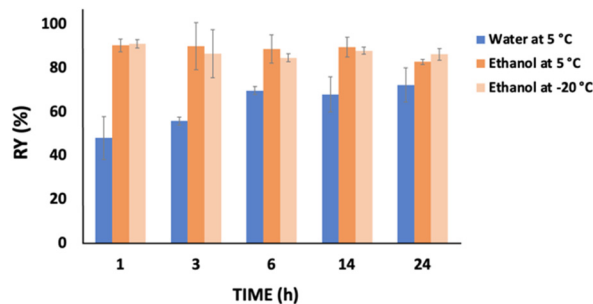


Fig. 3 Time effect on the keratin recovery yield.



was used as a coagulant agent, time appears to be an important factor, with the keratin recovery yield significantly increasing (~20 wt%; from 47.93 to 69.54 wt%) during the first six hours. Nevertheless, no significant differences were observed at time periods higher than 6 h.

All the previous results show that ethanol is the best coagulant agent, under the following operating conditions (time, temperature, and solution : coagulant ratio): 1 h, 5 °C, and 1 : 2 w/w. Under these conditions, the keratin recovery yield was (90 ± 3) wt%, which is a high yield, obtained using an amenable solvent and coagulant. Maity *et al.*⁴⁴ used 1 mL of aqueous solution (25 wt%) of tetramethyl ammonium hydroxide (TMAOH) to gradually dissolve chicken feathers (10 to 600 mg), achieving a partial dissolution (~60 wt%) in 6 h. The keratin recovery yield was (72 ± 2) wt%, achieved by adding acetic acid and acetone (1 : 4).⁴⁴ Furthermore, Pourjavaheri *et al.*¹² achieved a keratin yield of ~88 wt% using sodium sulfide and ~66 wt% using a solution of urea and L-cysteine, respectively. Fagbemi *et al.*⁴⁵ used sodium hydroxide (1.78%) and sodium bisulfite (0.5%), leading to a protein recovery yield of 65.21%.⁴⁵ Despite their lower recovery yields, it is relevant to highlight that these methods include dialysis for keratin recovery^{1,15,28} and long processing time (~3 days), while being necessary to change the water 3 times a day.

Keratin characterization

Keratin samples obtained under the different recovery conditions were analyzed by FTIR, SDS-PAGE, and TGA to determine their physicochemical properties and possible IL contaminations.

From Fig. S1 in the ESI† it is possible to observe the essential peaks in the keratin samples obtained under different conditions (coagulant, solution : coagulant ratio, temperature and time), corresponding to the stretching vibrations of O–H and N–H (Amide A) at 3650–2830 cm^{−1}, C=O stretching (Amide I) at 1735–1600 cm^{−1}, N–H bending and C–H stretching (Amide II) at 1600–1480 cm^{−1}, and amide III (1300–1200 cm^{−1}), being in agreement with the literature.^{46,47} The same peaks are observed for the remaining samples with the remaining studied variables, except for the use of ethanol at 1 : 5 w/w solution : coagulant ratio. From the FTIR spectra investigating the influence of the amount of ethanol (Fig. 4), the absorption peaks obtained for chicken feathers, ethanol 1 : 1, 1 : 2, 1 : 3, and 1 : 5 correspond to 1627 cm^{−1}, 1640 cm^{−1}, 1620 cm^{−1}, 1642 cm^{−1}, and 1630 cm^{−1} for Amide I; 1616 cm^{−1}, 1550 cm^{−1}, 1554 cm^{−1}, 1550 cm^{−1}, and 1512 cm^{−1} for Amide II; and 1227 cm^{−1}, 1232 cm^{−1}, 1231 cm^{−1}, 1246 cm^{−1}, and 1226 cm^{−1} for Amide III, respectively. Significant peaks at 1390 cm^{−1} (O–H bending) and 1160 cm^{−1} (C–O stretching) are observed for the samples recovered with ethanol 1 : 1, 1 : 2, and 1 : 3 (*cf.* Fig. 4), indicating IL presence in the keratin sample. These results highlight that a higher amount of coagulant during the recovery step is more efficient for IL removal.

The molecular weight of keratin samples obtained under different recovery conditions was analyzed by SDS-PAGE, showing a band around 5–12 kDa (*cf.* Fig. S2 in the ESI†). This

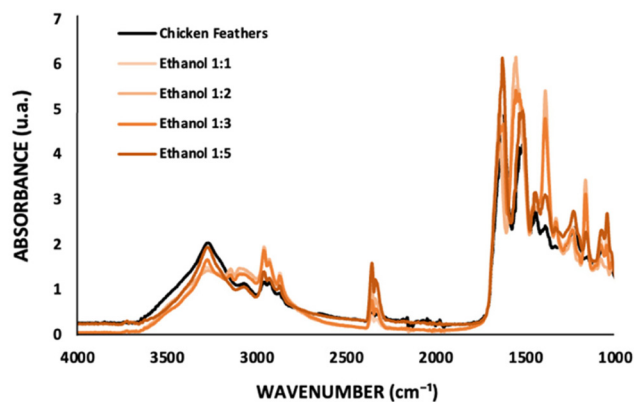


Fig. 4 FTIR spectra of chicken feathers and keratin samples recovered with ethanol at different solution : coagulant ratios.

is in accordance with the results reported in the literature for keratin from chicken feathers using other processing methods.^{3,12} Nevertheless, when acetone was used as a coagulant agent, no protein bands were identified in the electrophoresis gel, suggesting that the protein was degraded into lower molecular weight fractions, which are not possible to be identified in the gel.

A two-step degradation was observed in the TGA curves of both chicken feathers and recovered keratin samples (Fig. S3 in the ESI†). The first degradation step corresponds to water loss, occurring between 25 and 100 °C. The second stage of degradation of keratin polypeptides corresponds to the decomposition of disulfide bonds, resulting in the release of hydrogen sulfide and sulfur dioxide. Overall, the thermal stability assays of chicken feathers and recovered keratin samples showed that these biomaterials are stable up to 215 °C. The TGA results indicate that the recovered keratin has a similar profile to the original keratin in the feathers, being in agreement with the literature.^{21,48}

In general, no significant differences were observed in the keratin properties under the different recovery conditions, except for the improvement of the IL removal using a higher amount of ethanol and no identification of the protein band with the use of acetone as a coagulant agent.

IL recovery and reuse

Aiming to develop a sustainable process, [C₄C₁im][C₁CO₂] was recycled and reused three times with fresh chicken feathers. The results obtained are depicted in Fig. 5. All components of chicken feathers were dissolved into the IL aqueous solution (80 wt%, in a solid : liquid ratio of 1 : 20 w/w, at 100 °C, during 4 h), indicating that what was not recovered could be retained in the coagulant solvent, yet without significantly affecting the dissolution of chicken feathers and keratin recovery performance. Approximately 82% of the IL was recovered at the end of the third cycle, with the keratin yield decreasing only 4% from the first to the third cycle. This indicates that the reused IL does not significantly compromise the chicken feather dis-



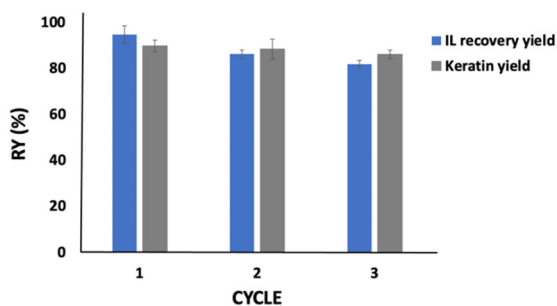


Fig. 5 IL and keratin recovery yield during three consecutive cycles.

solution and keratin recovery. As depicted in the ESI, in Fig. S5 to S8, ^1H and ^{13}C NMR spectra show that the IL maintains its structure, with no degradation, after the recovery step.

As shown in the FTIR results (*cf.* Fig. 4), a part of the IL is lost with the recovered protein. This may justify some of the IL losses observed here; however, it can also be related to losses during the whole process (*e.g.* during sample transfer between flasks). We would expect a higher recovery in a larger-scale industrial process, where surface losses are significantly lower. Besides, considering a higher volume of IL, we would expect more cycles to be successfully carried out. On the other hand, the washing step can improve the IL recovery, as reported by Zhang *et al.*,⁴⁹ who used $[\text{C}_2\text{C}_1\text{im}]\text{Cl}$ for cellulose regeneration. The authors recovered 71% of the IL after the first washing cycle, which improved to *ca.* 98% considering four washing cycles. In future work, we suggest an evaluation of several washing steps to improve the IL recovery and the techno-economic feasibility of this process applied at a large scale.

Film preparation and characterization

The best conditions (1 h, 5 °C, and ethanol 1:2 w/w) were used for keratin recovery. After the washing step, an aqueous solution of keratin (15 wt%) was prepared and heated at 60 °C for 30 min. Then, the solution was dried in a silicone molding at 50 °C for 24 h. A homogeneous, opaque, and yellow thin film was obtained (Fig. 6) and stored at 5 °C for further characterization. Mechanical and biological tests were performed to validate their future applications. To the best of our knowl-

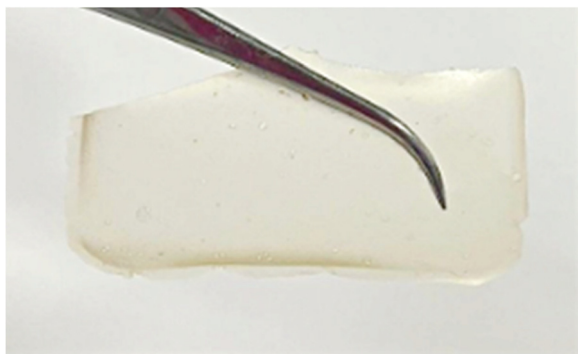


Fig. 6 Keratin film processed from chicken feathers waste.

edge, no previous results have been reported for keratin films obtained from chicken feathers processed with ILs. Therefore, these results can help to identify possible applications of this new biomaterial.

Film morphology

SEM was used to characterize the surface morphology of the keratin film. The topography of the keratin film (Fig. S4 in the ESI†) is smooth and homogeneous. The same morphology was observed by Nuutinen *et al.*,⁵⁰ who investigated the use of deep eutectic solvents in the processing of keratin films from feathers.

Film tensile strength

The tensile strength of the produced keratin film is 0.1289 ± 0.01 MPa, indicating that the film is fragile. The poor mechanical properties of this biomaterial is expected due to the low molecular weight of keratin.⁵⁰ Although not critical given the envisioned biomedical applications, to overcome this situation, cross-linking keratin (*e.g.*, glycerol) has been proposed and has shown excellent results.⁵⁰ Another option successfully reported in the literature is the addition of a biocompatible biopolymer, creating a blend, to improve the properties of the material.³⁵ In this regard, He *et al.*⁵¹ reported that the film's tensile strength was improved around five times by incorporating sodium alginate into the keratin film.

Contact angle

Contact angle measurements were performed to assess the hydrophilicity of the prepared keratin film. When water was used as a solvent, the drop quickly spread across the film, so measuring the contact angle was not possible. This happens because protein films are sensitive to water due to their hydrophilic nature.⁵⁰ Considering the higher density of ethylene glycol, it was successfully used to perform this analysis. The keratin film presented a contact angle of $52.77^\circ \pm 1.52^\circ$, characterizing it as hydrophilic ($\leq 90^\circ$). This characteristic can be related to the presence of the polar group at the film surface and the possibility of hydrogen-bonding. Analogously, Hamouche *et al.*⁵² prepared a wool keratin film and reported a contact angle of 53.5° , while Nuutinen *et al.*⁵⁰ prepared feathers keratin films and reported a contact angle of $45.84^\circ \pm 4.57^\circ$. In the literature, hydrophilic films have been positively investigated for biomedical applications.⁵³

In vitro cytotoxicity

Cytotoxicity tests have been successfully used as an initial step for bio-safety testing and the identification of potential toxicity of different biomaterials.⁵⁴ Aiming to evaluate the cytotoxicity of the prepared keratin film, some cells, namely macrophages, monocytes, keratinocytes, and fibroblasts, were used. In Fig. 7, the cytotoxicity results obtained are presented. Compared to the control, no significant impact was observed in the samples, indicating that the keratin film has no toxicity for these cells. Although there is no data in the literature about the cytotoxicity of keratin films from chicken feathers pro-



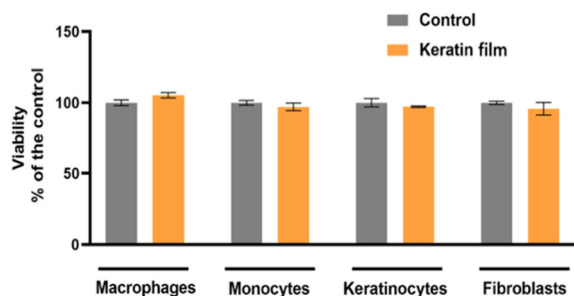


Fig. 7 Evaluation of keratin film's cell viability *in vitro* in macrophages, monocytes, keratinocytes, and fibroblasts.

cessed with ILs, the cytotoxicity of keratin from different sources and methods follows the findings of this work.⁵⁵ Overall, our results confirm that $[C_4C_1im][C_1CO_2]$ is efficient and safe to be applied in keratin biomaterial processing.

Anti-inflammatory and antioxidant effects of the keratin film

As LPS promotes an increase in nitrites – a stable metabolite of NO – production in macrophages, it has been used for the identification of the anti-inflammatory potential of compounds.⁵⁶ The main goal here was to identify whether macrophage exposure to the keratin film could induce NO production (Fig. 8A). Herein, the keratin film produced very low levels of nitriles (4.29), showing no significant differences with the control (1.01). This result indicates that the keratin film can inhibit nitrile production without affecting cell viability. With respect to ROS, representative images of fluorescence microscopy (Fig. 8B) show that the LPS induced a significant increase in ROS production. Images were acquired with an EVOS M5000 imaging system at 20× magnification (scale bar 100 μm). Interestingly, in the presence of the keratin film, similar levels of control were observed, indicating the antioxidant effect of this biomaterial.

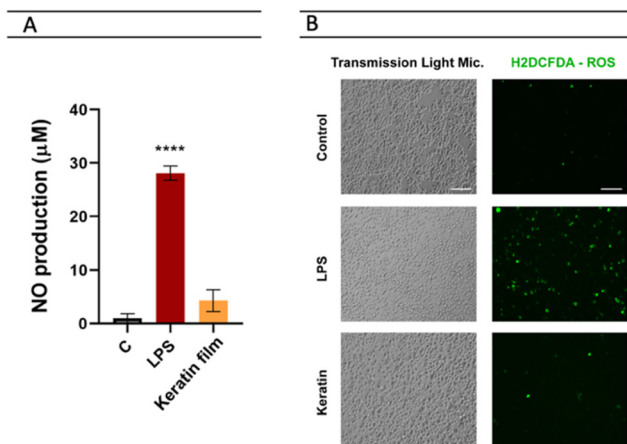


Fig. 8 Investigating the keratin film for (A) NO production and (B) oxidative stress.

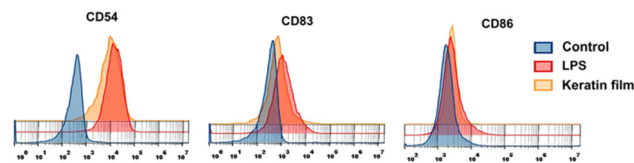


Fig. 9 Investigation of keratin film expression on different dendritic cells (CD54, CD83, and CD86).

Expression of the keratin film on the surface of dendritic cells (CDs)

As CDs are crucial components that contribute to the immune response,⁵⁷ we used CD54, CD83, and CD85 as activation marks and LPS as positive control to investigate whether the exposition of monocytes to the keratin film could promote any modifications in the immune response. According to the results presented in Fig. 9, the exposure of monocytes to the keratin film promotes an increase in the expression of some markers, namely CD83 (an activation marker) and CD54 (a molecule responsible for promoting adhesion between cells). Generally, it happens when cells are activated (pro-inflammatory stimulations). Considering this result, combined with the slight increase in NO observed in macrophages (Fig. 8A), we can suggest that the keratin film may promote slight activation of the innate immune response.

In vitro wound healing

Aiming to evaluate the wound healing effect and having in mind that cell migration is essential for wound contraction and the later curing stages, we investigated the ability of the prepared keratin film on keratinocytes (principal cell of the

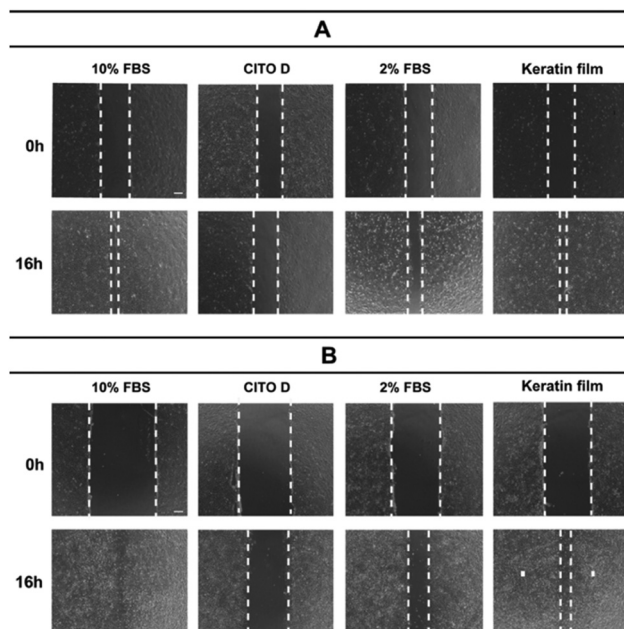


Fig. 10 The wound healing ability of keratin using (A) keratinocytes and (B) fibroblasts: an *in vitro* investigation.



epidermis) and fibroblasts (responsible cell for making the extracellular matrix) to speed up the closure of the wound. The results showed that the keratin film improves the proliferation of the cells, accelerating wound healing at 16 h (Fig. 10).

The mechanism of the wound healing ability of keratin is associated with keratin-cell interaction and amino acid sequences of RGD (arginine-glycine-aspartic acid) and LDV (leucine-aspartic acid-valine). These amino acids promote cellular attachment, migration, and proliferation during the healing process; however, the definite molecular mechanism remains unclear.^{58,59} Future investigations are necessary to clarify the molecular mechanism and assess the possible use of keratin for biomedical applications. In addition, wound healing studies have been carried out with a focus on human hair and wool keratins, leaving chicken feathers, which are a more abundant source than wool, and easier to control than human hair due to perming and coloring-dyeing,⁶⁰ underexplored.

Conclusions

Herein, the valorization of chicken feather waste by keratin recovery with ILs was demonstrated. More precisely, an aqueous solution of $[C_4C_1im][C_1CO_2]$ (80 wt%) was successfully used to achieve complete chicken feather dissolution at a solid : liquid ratio of 1 : 20 w/w within a short dissolution time (4 h) at 100 °C. Optimum recovery conditions were identified at 1 h, 5 °C, and using ethanol in a ratio of 1 : 2 w/w, achieving a keratin recovery yield of 90.17 wt%, with good physico-chemical properties.

The IL was successfully recycled and reused three times, and ~82 wt% of the IL was recovered at the end of the third cycle. We expect a higher recovery in an industrial process, where surface losses are significantly lower and more cycles can be successfully realized.

Using the optimal operating conditions, a keratin film (15 wt%) was prepared, and its properties were evaluated. In summary, a hydrophilic and homogeneous film was successfully prepared. As future work, the optimization of the keratin film processing, particularly to improve its tensile strength, is essential. Its cytotoxicity was investigated in macrophages, monocytes, keratinocytes, and fibroblasts. The keratin film did not present any cytotoxicity for these cells. Satisfactory results of anti-inflammatory activity were obtained. In addition, the *in vitro* wound healing study showed that the keratin film improves the proliferation of keratinocytes and fibroblasts, accelerating wound healing at 16 h.

The availability and low cost of keratin, when obtained from industrial waste, and its biochemical and physical properties are remarkable advantages. As future steps, evaluating the economic viability and investigating the molecular mechanism of keratin films in promoting wound healing are essential. The biorefinery concept presented herein is sustainable and can be extended to other keratin-based waste.

Author contributions

Conceptualization, C. P., H. P., J. A. P. C. and M. G. F.; methodology, C. P. and B. N.; writing – original draft preparation, C. P.; writing – review and editing, H. P., B. N., J. A. P. C. and M. G. F.; supervision, H. P. and M. G. F.; funding acquisition, M. G. F.; project administration, M. G. F. All authors listed have made a substantial, direct, and intellectual contribution to the work and have agreed to the published version of the manuscript.

Conflicts of interest

There are no conflicts to declare.

Acknowledgements

This work was developed within the scope of the project CICECO-Aveiro Institute of Materials, UIDB/50011/2020, UIDP/50011/2020 & LA/P/0006/2020, financed by national funds through the FCT/MCTES (PIDDAC). This work was funded by FEDER, through COMPETE2020 – Programa Operacional Competitividade e Internacionalização (POCI), and by national funds (OE), through FCT/MCTES, from the project POCI-01-0145-FEDER-031106 (IonCytDevice). C. Polesca acknowledges FCT – Fundação para a Ciência e a Tecnologia for the Ph.D. grant with the reference UI/BD/151282/2021. H. Passos acknowledges FCT, I.P., for the researcher contract CEECIND/00831/2017, under the Scientific Employment Stimulus-Individual Call, 2017.

References

- 1 S. Isarankura Na Ayutthaya, S. Tanpichai and J. Wootthikanokkhan, *J. Polym. Environ.*, 2015, **23**, 506–516.
- 2 B. Y. Alashwal, A. Gupta and M. S. B. Husain, *IOP Conf. Ser.: Mater. Sci. Eng.*, 2019, **702**, 1–7.
- 3 N. B. Kamarudin, S. Sharma, A. Gupta, C. G. Kee, S. M. S. B. T. Chik and R. Gupta, *3 Biotech*, 2017, **7**, 1–9.
- 4 T. Tesfaye, B. Sithole and D. Ramjugernath, *Sustainable Chem. Pharm.*, 2018, **8**, 38–49.
- 5 T. Upcraft, W. C. Tu, R. Johnson, T. Finnigan, N. van Hung, J. Hallett and M. Guo, *Green Chem.*, 2021, **23**, 5150–5165.
- 6 B. Mu, F. Hassan and Y. Yang, *Green Chem.*, 2020, **22**, 1726–1734.
- 7 M. Zhan and R. P. Wool, *J. Appl. Polym. Sci.*, 2016, **44013**, 1–7.
- 8 A. R. Aboulela, S. Y. Tan, G. H. Kelsall and J. P. Hallett, *ACS Sustainable Chem. Eng.*, 2020, **8**, 14441–14461.
- 9 T. Tesfaye, B. Sithole, D. Ramjugernath and V. Chunilall, *Waste Manage.*, 2017, **68**, 626–635.
- 10 X. Liu, Y. Nie, Y. Liu, S. Zhang and A. L. Skov, *ACS Sustainable Chem. Eng.*, 2018, **6**, 17314–17322.



- 11 C. R. Chilakamarthy, S. Mahmood, S. N. B. M. Saffe, M. A. B. Arifin, A. Gupta, M. Y. Sikkandar, S. S. Begum and B. Narasaiah, *3 Biotech*, 2021, **11**, 1–12.
- 12 F. Pourjavaheri, S. O. Pour, O. A. H. Jones, P. M. Smooker, R. Brkljača, F. Sherkat, E. W. Blanch, A. Gupta and R. A. Shanks, *Process Biochem.*, 2019, **82**, 205–214.
- 13 E. M. Nuutinen, P. Willberg-Keyriläinen, T. Virtanen, A. Mija, L. Kuutti, R. Lantto and A. S. Jääskeläinen, *RSC Adv.*, 2019, **9**, 19720–19728.
- 14 R.-R. Yan, J.-S. Gong, C. Su, Y.-L. Liu, J.-Y. Qian, Z.-H. Xu and J.-S. Shi, *Appl. Microbiol. Biotechnol.*, 2022, **106**, 2349–2366.
- 15 M. Borrelli, N. Joepen, S. Reichl, D. Finis, M. Schoppe, G. Geerling and S. Schrader, *Biomaterials*, 2015, **42**, 112–120.
- 16 N. Ramakrishnan, S. Sharma, A. Gupta and B. Y. Alashwal, *Int. J. Biol. Macromol.*, 2018, **111**, 352–358.
- 17 R. Li and D. Wang, *J. Appl. Polym. Sci.*, 2013, **127**, 2648–2653.
- 18 B. Ma, Q. Sun, J. Yang, J. Wizi, X. Hou and Y. Yang, *Environ. Sci. Pollut. Res.*, 2017, **24**, 17711–17718.
- 19 R. K. Donato and A. Mija, *Polymers*, 2020, **12**, 1–64.
- 20 A. Shavandi, T. H. Silva, A. A. Bekhit and A. E. D. A. Bekhit, *Biomater. Sci.*, 2017, **5**, 1699–1735.
- 21 A. Idris, R. Vijayaraghavan, U. A. Rana, D. Fredericks, A. F. Patti and D. R. MacFarlane, *Green Chem.*, 2013, **15**, 525–534.
- 22 A. Idris, R. Vijayaraghavan, U. A. Rana, A. F. Patti and D. R. MacFarlane, *Green Chem.*, 2014, **16**, 2857–2864.
- 23 Y. Ji, J. Chen, J. Lv, Z. Li, L. Xing and S. Ding, *Sep. Purif. Technol.*, 2014, **132**, 577–583.
- 24 Y. J. Yang, D. Ganbat, P. Aramwit, A. Bucciarelli, J. Chen, C. Migliaresi and A. Motta, *EXPRESS Polym. Lett.*, 2019, **13**, 97–108.
- 25 H. Xie, S. Li and S. Zhang, *Green Chem.*, 2005, **7**, 606–608.
- 26 X. Liu, Y. Nie, X. Meng, Z. Zhang, X. Zhang and S. Zhang, *RSC Adv.*, 2017, **7**, 1981–1988.
- 27 Z. Zhang, Y. Nie, Q. Zhang, X. Liu, W. Tu, X. Zhang and S. Zhang, *ACS Sustainable Chem. Eng.*, 2017, **5**, 2614–2622.
- 28 A. Aluigi, C. Tonetti, F. Rombaldoni, D. Puglia, E. Fortunati, I. Armentano, C. Santulli, L. Torre and J. M. Kenny, *J. Mater. Sci.*, 2014, **49**, 6257–6269.
- 29 C. Apostolidou, *ChemistryOpen*, 2020, **9**, 695–702.
- 30 S. P. M. Ventura, F. A. E. Silva, M. v. Quental, D. Mondal, M. G. Freire and J. A. P. Coutinho, *Chem. Rev.*, 2017, **117**, 6984–7052.
- 31 Z. Zhang, Y. Nie, Q. Zhang, X. Liu, W. Tu, X. Zhang and S. Zhang, *ACS Sustainable Chem. Eng.*, 2017, **5**, 2614–2622.
- 32 S. Zheng, Y. Nie, S. Zhang, X. Zhang and L. Wang, *ACS Sustainable Chem. Eng.*, 2015, **3**, 2925–2932.
- 33 Y. X. Wang and X. J. Cao, *Process Biochem.*, 2012, **47**, 896–899.
- 34 N. A. Samsudin, F. W. Low, Y. Yusoff, M. Shakeri, X. Y. Tan, C. W. Lai, N. Asim, C. S. Oon, K. S. Newaz, S. K. Tiong and N. Amin, *J. Mol. Liq.*, 2020, **308**, 113030–113037.
- 35 C. Polesca, H. Passos, J. A. P. Coutinho and M. G. Freire, *Curr. Opin. Green Sustainable Chem.*, 2022, **37**, 100675–100683.
- 36 A. Rivera-Galletti, C. R. Gough, F. Kaleem, M. Burch, C. Ratcliffe, P. Lu, D. S. L. Cruz and X. Hu, *Polymers*, 2021, **13**, 2911–2921.
- 37 Y. Hu, L. Liu, W. Dan, N. Dan and Z. Gu, *J. Appl. Polym. Sci.*, 2013, **130**, 2245–2256.
- 38 A. Idris, R. Vijayaraghavan, A. F. Patti and D. R. Macfarlane, *ACS Sustainable Chem. Eng.*, 2014, **2**, 1888–1894.
- 39 J. O'Brien, I. Wilson, T. Orton and F. Pognan, *Eur. J. Biochem.*, 2000, **267**, 5421–5426.
- 40 H. Passos, T. B. V. Dinis, A. F. M. Cláudio, M. G. Freire and J. A. P. Coutinho, *Curr. Opin. Green Sustainable Chem.*, 2018, **20**, 14234–14241.
- 41 M. A. R. Martins, F. H. B. Sosa, I. Kilpeläinen and J. A. P. Coutinho, *Fluid Phase Equilib.*, 2022, **556**, 113414–113423.
- 42 X. Zhang, Y. Feng and X. Yang, *Fibers Polym.*, 2021, **22**, 3326–3335.
- 43 I. Khan, M. L. S. Batista, P. J. Carvalho, L. M. N. B. F. Santos, J. R. B. Gomes and J. A. P. Coutinho, *J. Phys. Chem. B*, 2015, **119**, 10287–10303.
- 44 T. K. Maity, N. Singh, P. Vaghela, A. Ghosh, S. Singh, P. B. Shinde, R. A. Sequeira and K. Prasad, *Sustainable Environ. Res.*, 2022, **32**, 1–8.
- 45 O. D. Fagbemi, B. Sithole and T. Tesfaye, *Sustainable Chem. Pharm.*, 2020, **17**, 100267–100278.
- 46 O. L. Shanmugasundaram, K. S. Z. Ahmed, K. Sujatha, P. Ponnmurugan, A. Srivastava, R. Ramesh, R. Sukumar and K. Elanithi, *Mater. Sci. Eng., C*, 2018, **92**, 26–33.
- 47 B. Ma, X. Qiao, X. Hou and Y. Yang, *Int. J. Biol. Macromol.*, 2016, **89**, 614–621.
- 48 S. Alahyaribeik and A. Ullah, *Int. J. Biol. Macromol.*, 2020, **148**, 449–456.
- 49 H. Zhang, A. Ionita, P. F. Serinán, M. L. Ferrer, M. A. Rodríguez, A. Tamayo, F. R. Alons, F. del Monte and M. C. Gutiérrez, *Molecules*, 2022, **27**, 987–999.
- 50 E. M. Nuutinen, T. Virtanen, R. Lantto, M. Vähä-Nissi and A. S. Jääskeläinen, *RSC Adv.*, 2021, **11**, 27512–27522.
- 51 M. He, B. Zhang, Y. Dou, G. Yin and Y. Cui, *J. Appl. Polym. Sci.*, 2017, **44680**, 1–8.
- 52 H. Hamouche, S. Makhoul, A. Chaouchi and M. Laghrouche, *Sens. Actuators, A*, 2018, **282**, 132–141.
- 53 D. Ahmad, I. van den Boogaert, J. Miller, R. Presswell and H. Jouhara, *Energy Sources Part A*, 2018, **40**, 2686–2725.
- 54 F. Soheilmoghaddam, G. Sharifzadeh, H. Adelnia and M. U. Wahit, *J. Polym. Environ.*, 2021, **30**, 613–621.
- 55 G. J. Dias, T. N. Haththotuwa, D. S. Rowlands, M. Gram and A. E. D. A. Bekhit, *Food Chem.*, 2022, **383**, 132436–132468.
- 56 S. N. Pedro, M. S. M. Mendes, B. M. Neves, I. F. Almeida, P. Costa, I. Correia-Sá, C. Vilela, M. G. Freire, A. J. D. Silvestre and C. S. R. Freire, *Pharmaceutics*, 2022, **14**, 827–844.



- 57 E. S. Reis, J. A. M. Barbuto, J. Köhl and L. Isaac, *Mol. Immunol.*, 2008, **45**, 1952–1962.
- 58 Y. Chen, Y. Li, X. Yang, Z. Cao, H. Nie, Y. Bian and G. Yang, *Acta Biomater.*, 2021, **125**, 208–218.
- 59 R. R. Yan, J. S. Gong, C. Su, Y. L. Liu, J. Y. Qian, Z. H. Xu and J. S. Shi, *Appl. Microbiol. Biotechnol.*, 2022, **106**, 2349–2366.
- 60 J. Wang, S. Hao, T. Luo, Z. Cheng, W. Li, F. Gao, T. Guo, Y. Gong and B. Wang, *Colloids Surf., B*, 2017, **149**, 341–350.

